

Supplementary Information

Penicillamine-Protected Ag₂₀ Nanoclusters and the Fluorescence Chemosensing for Trace Detection of Copper Ions

Xianhu Liu,^{†,‡,§} Weihua Ding,^{†,§} Yishi Wu,[†] Chenghui Zeng,[†] Zhixun Luo,^{*,†}
Hongbing Fu^{*,†}

[†]State Key Laboratory for Structural Chemistry of Unstable and Stable Species,
Institute of Chemistry, Chinese Academy of Sciences, Beijing, 100190, P. R. China

[‡]Department of Chemistry, Huaibei Normal University, Huaibei, Anhui 235000, P. R.
China

[§]These authors contribute equally to this paper and share the first authorship.

S1. Materials

Silver nitrate (AgNO_3 , > 99.999%), D-penicillamine (99%, DPA), Sodium borohydride (99%, NaBH_4), α -Cyano-4-hydroxycinnamic acid (98%, CHCA) and 1-hydroxyethylidene-1, 1-diphosphonicacid (60% wt%, HEDP) were obtained from J&K Scientific Ltd. (Beijing, China). Methanol and ethanol were purchased from Sinopharm Chemical Reagent Co., Ltd. (HPLC, Beijing, China). Ultrapure water (18.2 M Ω) was used in all experiments.

S2. Absorption of the silver nanoclusters (Ag NCs)

In the process of preparing Ag NCs by size-focusing methods, one critical factor is the S/Ag ratio. We have inspected the ratios of S/Ag from 2 to 7 and the absorption spectra were almost featureless (**Figure S1**) except that the ratio of S/Ag is 4.

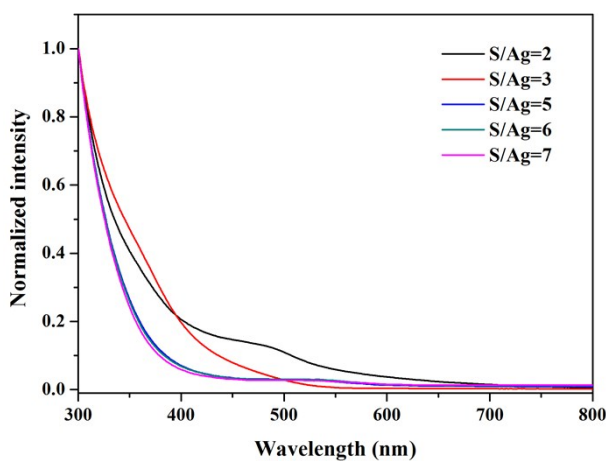


Figure S1. UV-vis absorption spectra of the products at different S/Ag ratios.

S3. Mass spectra of the Ag NCs at low mass range

In addition the mass spectra provided in the main text showing a mass range ~2000-7000 amu, here we also provide the MALDI-TOF MS at the low mass range <2000. As shown in Figure S3, there are a few peaks appearing at 861, 691 and 656 amu corresponding to the fragment ions of the Ag₂₀ NCs.

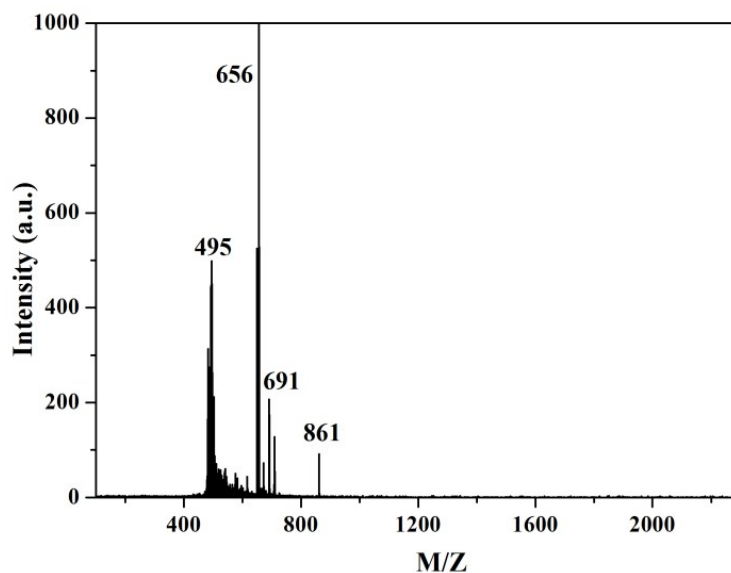


Figure S2. MALDI TOF MS of the Ag NCs in the mass range of 200 to 2000.

S4. TD-DFT calculation of absorption spectrum

The ligands of the $\text{Ag}_{20}(\text{DPA})_{18}$ NCs were replaced by $-\text{SCH}_3$ to facilitate the computation. Geometries were optimized using b3lyp/sto-3g method and basis set. After obtaining the optimized ground state isomers, we calculated the single point energy using b3lyp/lanl2dz method and basis set involved in the Gaussian 09 software. The absorption spectrum was computed on the basis of time-dependent density functional theory (TD-DFT).

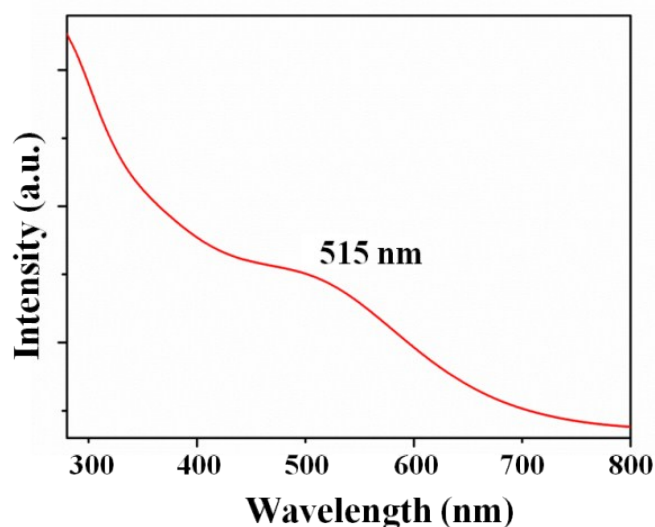


Figure S3. The optical absorption spectrum of $\text{Ag}_{20}(\text{SCH}_3)_{18}$ by computation.

S5. Fluorescence of silver nanoclusters (Ag NCs)

The fluorescence spectra of the Ag NCs under different pH solutions were measured (Figure S4). It was found that the fluorescence intensity of NCs is very sensitive to the pH values and the intensity increase to the maximum value when the pH is 3.5.

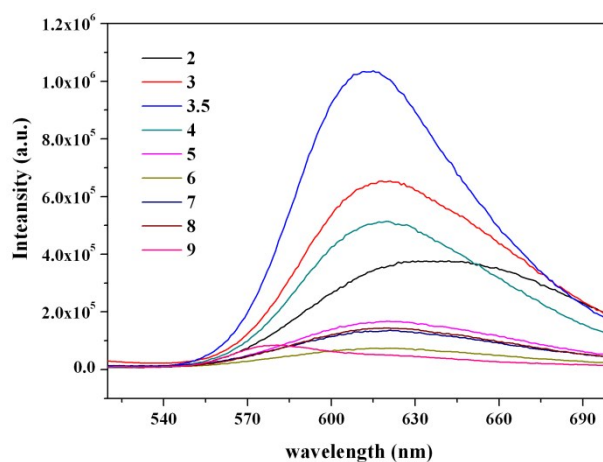


Figure S4. The fluorescence spectra of the Ag NCs at different pH values.

S6. Ions detection

The water soluble Ag NCs were used to detect the common metal ion in aqueous solution and it was found that the fluorescence was quenched greatly after the addition of copper ion as the strong interaction effects between DPA and copper ion. However, the addition of Fe^{3+} also decreased the fluorescence of Ag NCs to a certain degree (**Figure S5**). Thus, the chelating agent of 1-hydroxyethylidene-1, 1-diphosphonicacid (HEDP) was employed to eliminate interference from Fe^{3+} ion to improve the selectivity of our sensor towards Cu^{2+} ions.

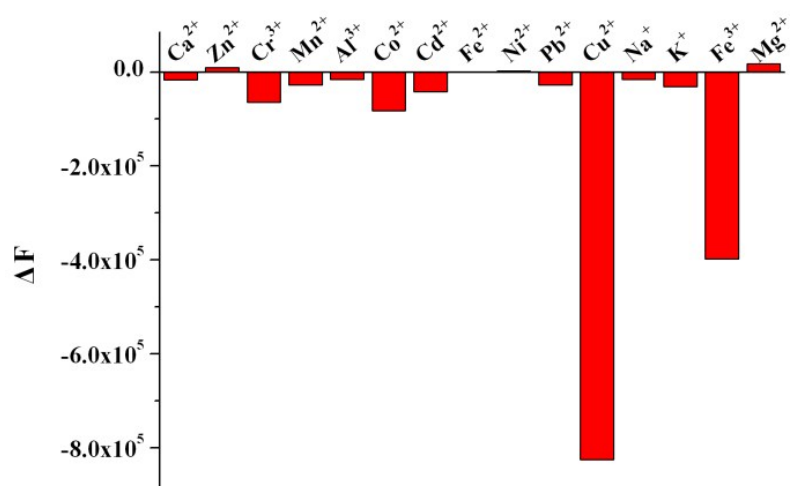


Figure S5. Selectivity of the Ag NCs sensor for Cu^{2+} ion detection by the fluorescence quenching strategy.

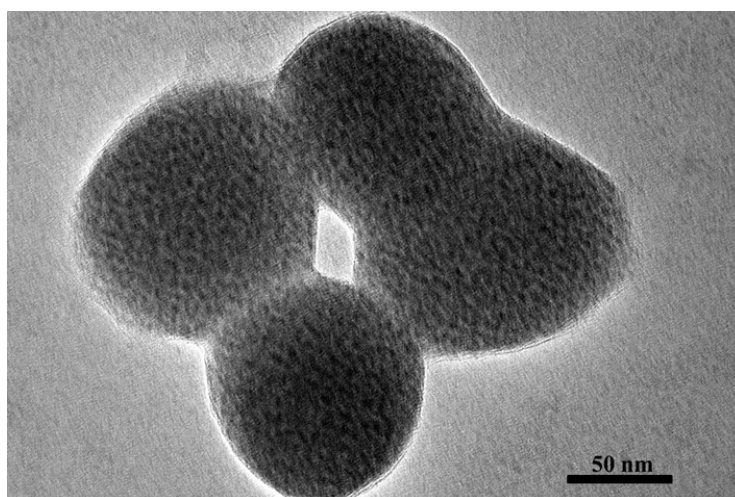


Figure S6. TEM picture of the silver NCs after addition of copper ion.

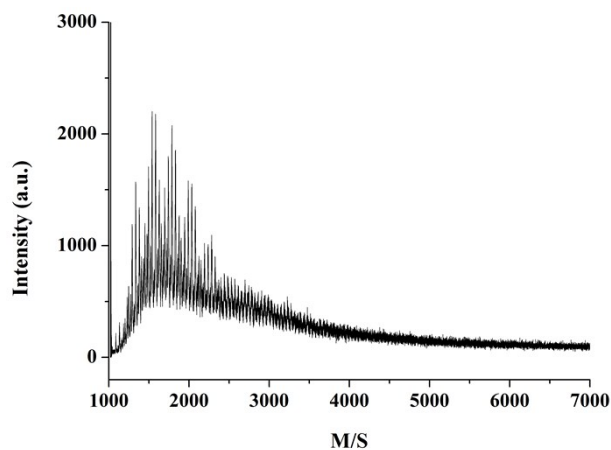


Figure S7. MALDI-TOF MS of the silver NCs after addition of copper ion.

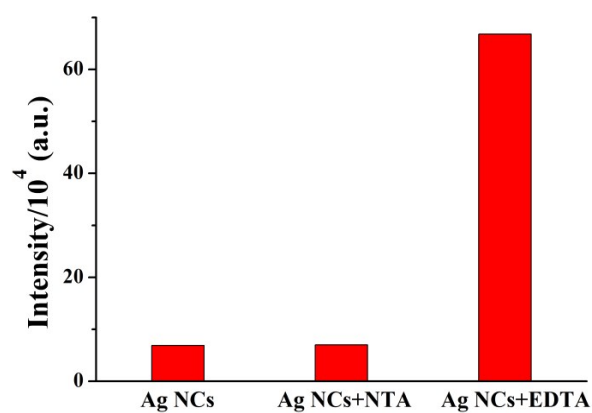


Figure S8. The variation of fluorescence of Ag_{20} NCs with different response to the chelating ligand of NTA and EDTA respectively in the absence of Cu^{2+} .

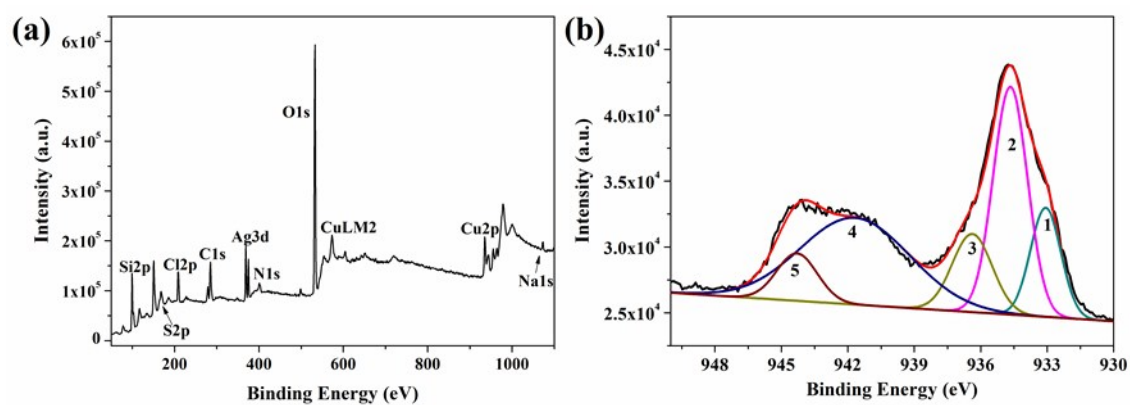
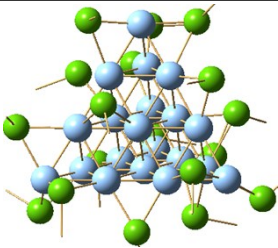
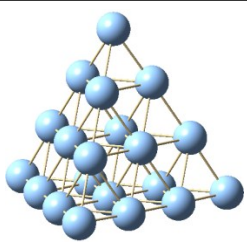


Figure S9. (a) XPS full spectra of the silver NCs after addition of copper ion, and (b) high-resolution XPS spectrum of the deconvoluted $\text{Cu}2p$ of Ag NCs-Cu^{2+} . The concentrations of Ag NCs and Cu^{2+} were 0.03 mg/mL and $0.1 \mu\text{M}$ respectively.

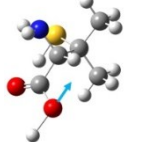
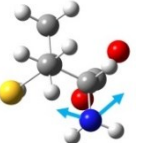
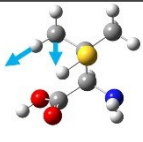
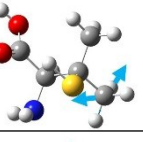
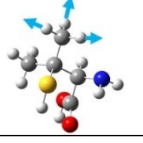
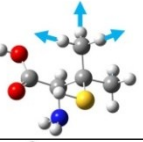
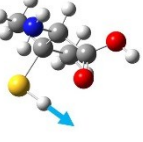
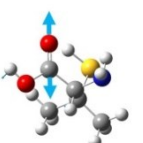
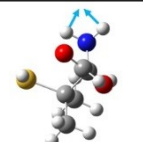
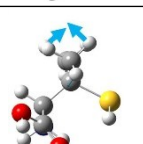
S7. Surface Charge Distribution

Table S1. The surface charge distributions of Ag_{20} core and $\text{Ag}_{20}(\text{SCH}_3)_{18}$.

	$\text{Ag}_{20}(\text{SCH}_3)_{18}$	Ag_{20} core
Structure		
Surface charge distributions	1 Ag -0.938886 2 Ag -0.338515 3 Ag -0.262761 4 Ag 0.264366 5 Ag -0.121382 6 Ag -0.989895 7 Ag -0.837919 8 Ag -0.782325 9 Ag -0.407293 10 Ag -0.566275 11 Ag -0.075316 12 Ag -0.453677 13 Ag -0.133950 14 Ag -0.305859 15 Ag 1.698630 16 Ag 1.313392 17 Ag 0.027588 18 Ag -0.242322 19 Ag -0.888483 20 Ag 2.024643	1 Ag 0.469285 2 Ag -0.009186 3 Ag -0.010754 4 Ag -0.010574 5 Ag -0.009623 6 Ag 0.469238 7 Ag 0.469234 8 Ag 0.469259 9 Ag -0.009670 10 Ag -0.010052 11 Ag -0.009609 12 Ag -0.008712 13 Ag -0.009831 14 Ag -0.009084 15 Ag -0.440193 16 Ag -0.440171 17 Ag -0.440283 18 Ag -0.009730 19 Ag -0.009264 20 Ag -0.440280

S8. FTIR and Raman Characterization

Table S2. The frequency of the vibration and related assignments for both FTIR and Raman spectra of DPA.

Wavenumber/cm ⁻¹	Character	Displacement vector
3743	O-H stretch	
3448	H-N-H Vs	
3172	H-C-H Vas	
2972	H-C-H Vas	
2925	H-C-H Vs	
2854	H-C-H Vs	
2511	O-H stretch	
1606	C=O stretch	
1525	H-N-H scissoring	
1465	H-C-H scissoring	

S9. Comparison of different detection methods

Table S3. Comparison of different detection methods for Cu²⁺ sensing

Detection methods	Detection limit	Linear range	References
Carbon dots-based	1 μM	1-100 μM	[1]
	35.2 nM	0 - 3 μM	[2]
	10 nM	1 - 100 μM	[3]
	5 nM	0 - 5 μM	[4]
	0.3 nM	0 - 600 nM	[5]
DNAzymes-based	5 μM	0.01 - 1 mM	[6]
	35 nM	35 nM - 20 μM	[7]
	4 nM	10 - 200 nM	[8]
Quantum dots-based	10 nM	1 - 100 μM	[9]
	1.1 nM	50 - 500 nM	[10]
Colorimetric	1 μM	10 - 150 μM	[11]
	290 nM	625 nM - 15 μM	[12]
Ag NCs-based	10 nM	0 - 1 μM	[13]
	10 nM	10 nM - 7.7 μM	[14]
	5 μM	5 - 150 μM	[15]
Our method	4 nM	16.7 nM - 7.2 μM	This work

References

- [1] A. Zhu, Q. Qu, X. Shao, B. Kong, Y. Tian, Carbon-dot-based dual-emission nanohybrid produces a ratiometric fluorescent sensor for in vivo imaging of cellular copper ions, *Angew. Chem. Int. Ed.* **2012**, *51*, 7185–7189.
- [2] X. Liu, N. Zhang, T. Bing, D. Shangguan, Carbon dots based dual-emission silica nanoparticles as a ratiometric nanosensor for Cu²⁺, *Anal. Chem.* **2014**, *86*, 2289-2296.
- [3] Q. Qu, A. Zhu, X. Shao, G. Shi, Y. Tian, Development of a carbon quantum dots based fluorescent Cu²⁺ probe suitable for living cell imaging, *Chem. Commun.* **2012**, *48*, 5473-5475.
- [4] Gedda, G.; Lee, C.-Y.; Lin, Y.-C.; Wu, H.-f., Green synthesis of carbon dots from prawn shells for highly selective and sensitive detection of copper ions. *Sensors Actuat. B-chem.* **2016**, *224*, 396-403.
- [5] Hou, J.; Zhou, T.; Wang, L.; Zhang, P.; Ding, L., Template-free microwave-assisted fabrication of carbon dots/Zn(OH)₂ composites for separation and enhancing chemical sensing. *Sensors Actuat. B-chem.* **2016**, *230*, 615-622.
- [6] J. Liu, Y. Lu, Colorimetric Cu²⁺ detection with a ligation DNAzyme and nanoparticles, *Chem. Commun.* **2007**, 4872-4874.

- [7] J. Liu, Y. Lu, A DNAzyme catalytic beacon sensor for paramagnetic Cu²⁺ ions in aqueous solution with high sensitivity and selectivity, *J. Am. Chem. Soc.* **2007**, *129*, 9838-9839.
- [8] Q. Zhang, Y. Cai, H. Li, D.-M. Kong, H.-X. Shen, Sensitive dual DNAzymes-based sensors designed by grafting self-blocked G-quadruplex DNAzymes to the substrates of metal ion-triggered DNA/RNA-cleaving DNAzymes, *Biosens. Bioelectron.* **2012**, *38*, 331-336.
- [9] Q. Qu, A. Zhu, X. Shao, G. Shi, Y. Tian, Development of a carbon quantum dots based fluorescent Cu²⁺ probe suitable for living cell imaging, *Chem. Commun.* **2012**, 5473-5475.
- [10] J. Yao, K. Zhang, H. Zhu, F. Ma, M. Sun, H. Yu, J. Sun, S. Wang, Efficient ratiometric fluorescence probe based on dual-emission quantum dots hybrid for on-site determination of copper ions, *Anal. Chem.* **2013**, *85*, 6461-6468.
- [11] H. Chen, J. Zhang, X. Liu, Y. Gao, Z. Ye, G. Li, Colorimetric copper (II) ion sensor based on the conformational change of peptide immobilized onto the surface of gold nanoparticles, *Anal. Methods* **2014**, *6*, 2580-2585.
- [12] Yong, W.; Fan, Y.; Xiurong, Y., Label-free colorimetric biosensing of copper (II) ions with unimolecular self-cleaving deoxyribozymes and unmodified gold nanoparticle probes. *Nanotechnology* **2010**, *21*, 205502.
- [13] M. Zhang, B.-C. Ye, Label-free fluorescent detection of copper (II) using DNA templated highly luminescent silver nanoclusters, *Analyst* **2011**, *136*, 5139-5142.
- [14] Z. Yuan, N. Cai, Y. Du, Y. He, E.S. Yeung, Sensitive and selective detection of copper ions with highly stable polyethyleneimine-protected silver nanoclusters, *Anal. Chem.* **2014**, *86*, 419-426.
- [15] X. Liu, C. Zong, L. Lu, Fluorescent silver nanoclusters for user-friendly detection of Cu²⁺ on a paper platform, *Analyst* **2012**, *137*, 2406-2414.